Supporting Information

Nanoporous Platinum/$(Mn,Al)_3O_4$ Nanosheet Nanocomposites with Synergistically Enhanced Ultrahigh Oxygen Reduction Activity and Excellent Methanol Tolerance

Conghui Si, Jie Zhang, Ying Wang, Wensheng Ma, Hui Gao, Lanfen Lv, and Zhonghua Zhang*

Key Laboratory for Liquid-Solid Structural Evolution and Processing of Materials (Ministry of Education), School of Materials Science and Engineering, Shandong University, Jingshi Road 17923, Jinan, 250061, P.R. China

*Corresponding author. Email: zh_zhang@sdu.edu.cn (Z.H. Zhang).

ORR mechanism

There are two ORR pathways are usually considered in alkaline media:

(i) direct 4 e^- pathway

$$O_2 + 2H_2O + 4e^- \rightarrow 4OH^- \quad (1a)$$

(ii) indirect 2 e^- pathway

$$O_2 + H_2O + 2e^- \rightarrow HO_2^- + OH^- \quad (1b)$$

followed by either the further 2 e^- reduction of HO_2^-

$$HO_2^- + H_2O + 2e^- \rightarrow 3OH^- \quad (1c)$$

or the purely chemical decomposition reaction of HO_2^-

$$2HO_2^- \rightarrow 2OH^- + O_2 \quad (1d)$$

RHE conversion

A saturated calomel electrode (SCE) was used as the reference electrode in all measurements. The measured potentials versus the SCE reference electrode were converted to the reversible hydrogen electrode (RHE) scale via the Nernst equation:

$$E_{RHE} = E_{SCE} + 0.0591pH + E^0_{SCE} \quad (2)$$

where E_{RHE} is the converted potential versus RHE, E_{SCE} is the experimental potential measured against the SCE reference electrode, and E^0_{SCE} is the standard potential of SCE at 25 ℃ (0.2415 V). The electrochemical measurements were carried out in the 0.1 M KOH solution (pH = 13) at room temperature. Therefore, $E_{RHE} = E_{SCE} + 1.0098$ V.

iR-corrected potential

The iR-corrected potential, $E_{iR\text{-}corrected}$, calculated by the following equation:

$$E_{iR\text{-}corrected} = E_{applied} - iR \quad (3)$$

where $E_{applied}$ is the applied potentials, i is the current and R is the uncompensated ohmic electrolyte resistance ($\approx$40 Ω) measured via high frequency AC impedance in the O_2-saturated 0.1 M KOH solution.

The adsorption energy (E_{ads}) calculation:

After attaining the optimized structures, the adsorption energy of molecules on the substrate was obtained. The E_{ads} was calculated by the following equation:

$$E_{ads} = E_{adsorbate} + E_{substrate} - E_{adsorbate/substrate} \quad (4)$$

where $E_{adsorbate}$ and $E_{substrate}$ correspond to the energy of the adsorbate isolated with substrate and the energy of the substrate respectively, $E_{adsorbate/substrate}$ is the total energy of adsorbate/substrate system. By this definition, a positive value of E_{ads} corresponds to an exothermic process, indicating that the adsorbate molecule would be easily adsorbed to the surface of the substrate.

Electrochemically active surface area (*ECSA*) calculation

The *ECSA* of a catalyst containing Pt can be calculated according to the following equation:

$$ECSA_{Pt}\ (m^2 g^{-1}) = Q_H/(2.1 \times m_{Pt}) \quad (5)$$

where Q_H (C) is the charge exchanged during hydrogen desorption on the surface, and

m_{Pt} (g) is the amount of Pt loaded on the working electrode.

Mass activity calculation

The mass activity of the catalyst was calculated via the following equation:

$$Mass\ activity = I/m \quad (6)$$

in which I is the reaction current of the catalyst at 0.9 or 0.85 V vs. RHE and m is the amount of Pt loading on the GC electrode.

The transferred electron number (n) calculation

The ORR kinetics of the prepared catalyst has been studied with the rotating disk electrode (RDE) measurement. The transferred electron number (n) was calculated via the Koutecky-Levich equations:

$$1/J = 1/J_L + 1/J_K = 1/B\omega^{1/2} + 1/J_K \quad (7a)$$

$$B = 0.62nFkD_0^{2/3}v^{-1/6}C_0 \quad (7b)$$

$$J_K = nFkC_0 \quad (7c)$$

in which J, J_K, and J_L correspond to the measured current density, the kinetic current density and diffusion-limiting current density respectively, B is a constant as a function of the concentration, diffusion coefficient of O_2 in the electrolyte and viscosity of the electrolyte, n is the transferred electron number, F is the Faraday constant (96485 C mol^{-1}), D_0 is the diffusion coefficient of O_2 in the 0.1 M KOH solution (1.9×10^{-5} cm^2 s^{-1}), ω is the angular velocity of the disk ($\omega=2\pi N$, N is the linear rotation speed), v is the kinetic viscosity of the electrolyte (0.01 cm^2 s^{-1}), C_0 is

the bulk concentration of O_2 (1.2×10^{-3} mol cm^{-3}), k is the electron transfer rate constant.

Calculation of the transferred electron number and peroxide (H_2O_2) yield based upon the RRDE data

The peroxide yield and the transferred electron number (n) were calculated from the RRDE data via the following equations:

$$\%\ (H_2O_2) = 200I_{ring}/(I_{disk}N + I_{ring}) \quad (8a)$$

$$n = 4I_{disk}N/(I_{disk}N + I_{ring}) \quad (8b)$$

where I_{ring} is the ring current, I_{disk} is the disk current and N is the current collection efficiency of the Pt ring. N was determined to be 0.37 from the reduction of $K_3Fe[CN]_6$.

Supplementary Figures (Figure S1 - S20)

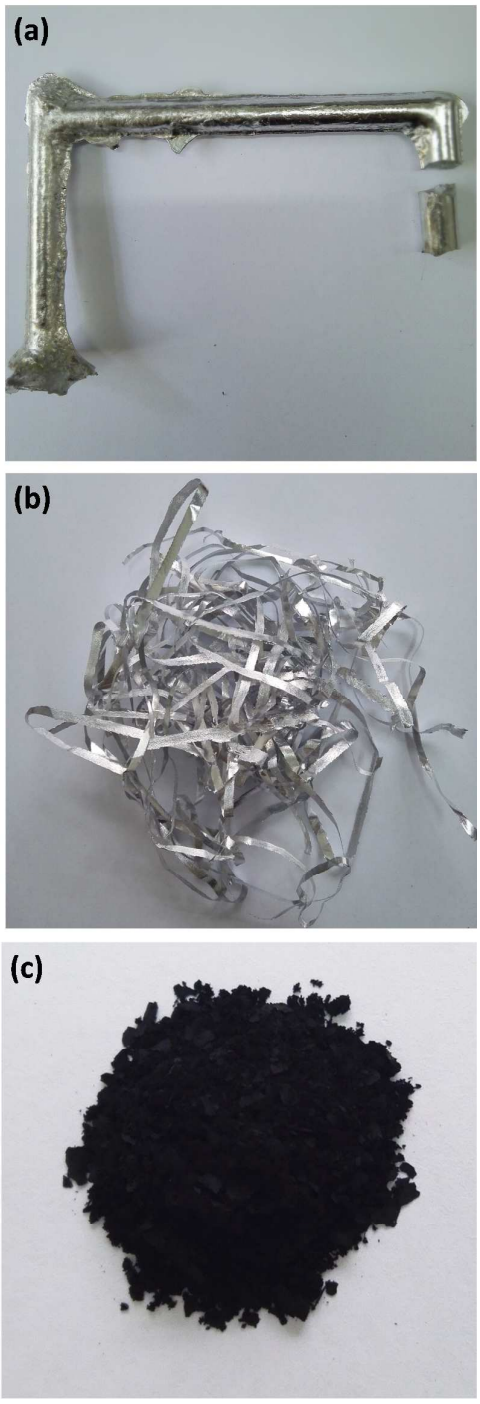

Figure S1. Macrographs of (a) the $Al_{94.8}Mn_5Pt_{0.2}$ ingot (mass: around 80 g), (b) the $Al_{94.8}Mn_5Pt_{0.2}$ foils and (c) the final np-Pt/$(Mn,Al)_3O_4$ NS powders. A large amount of catalysts could be fabricated using this strategy.

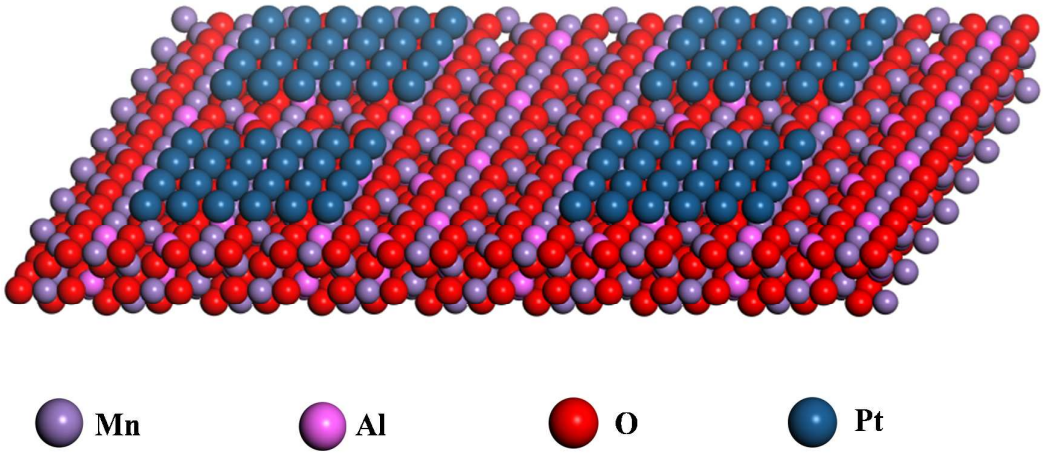

Figure S2. The atomic structure of np-Pt/$(Mn,Al)_3O_4$ NS, which contains monolayer Pt atoms supported on the $(Mn,Al)_3O_4$ (110) substrate.

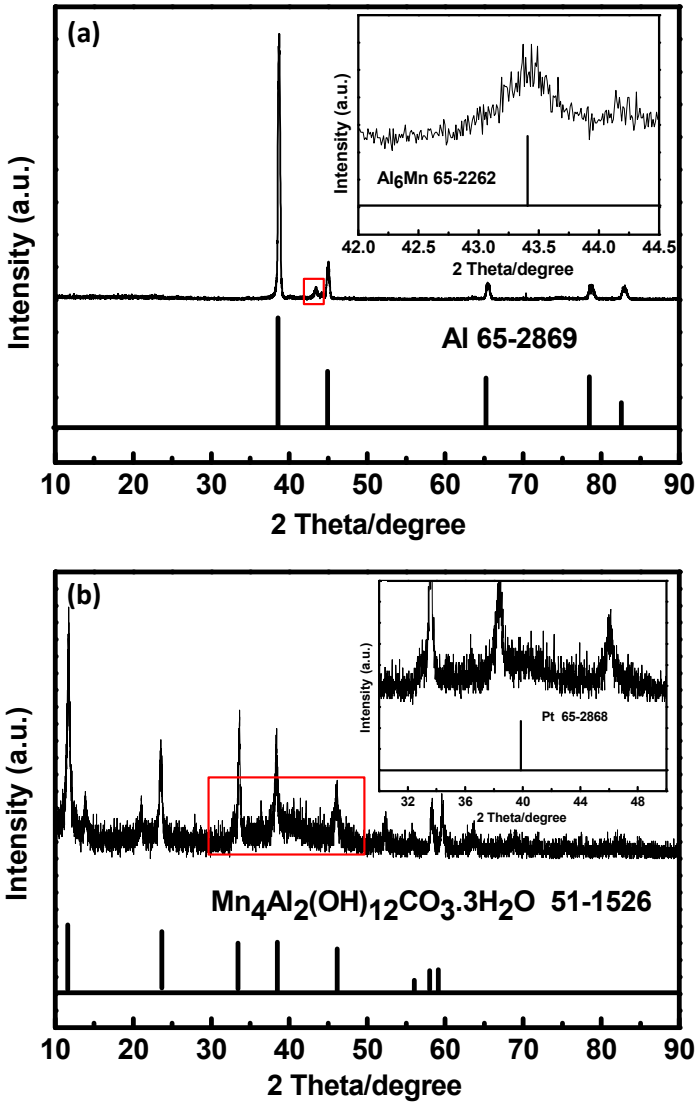

Figure S3. (a) XRD pattern of the $Al_{94.8}Mn_5Pt_{0.2}$ precursor foils which confirms the formation of the Al_6Mn and Al phases, inset: an enlarged part of the XRD pattern. (b) XRD pattern of the as-dealloyed sample after dealloying in a 2 M NaOH solution which confirms the formation of the $Mn_4Al_2(OH)_{12}CO_3 \cdot 3H_2O$ and Pt phases, inset: an enlarged part of the XRD pattern.

In **Figure S3b**, the broad peak located at 39.8° agrees well with the (111) reflection of the f.c.c. Pt phase (JCPDS 65-2868, inset of **Figure S3b**)

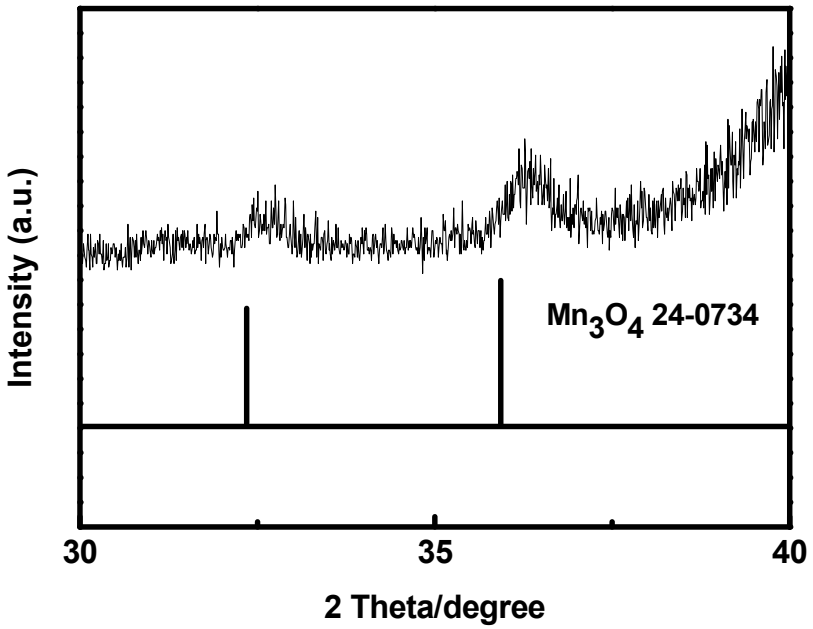

Figure S4. An enlarged part of the XRD pattern for the np-Pt/$(Mn,Al)_3O_4$ NS sample (**Figure 1a**).

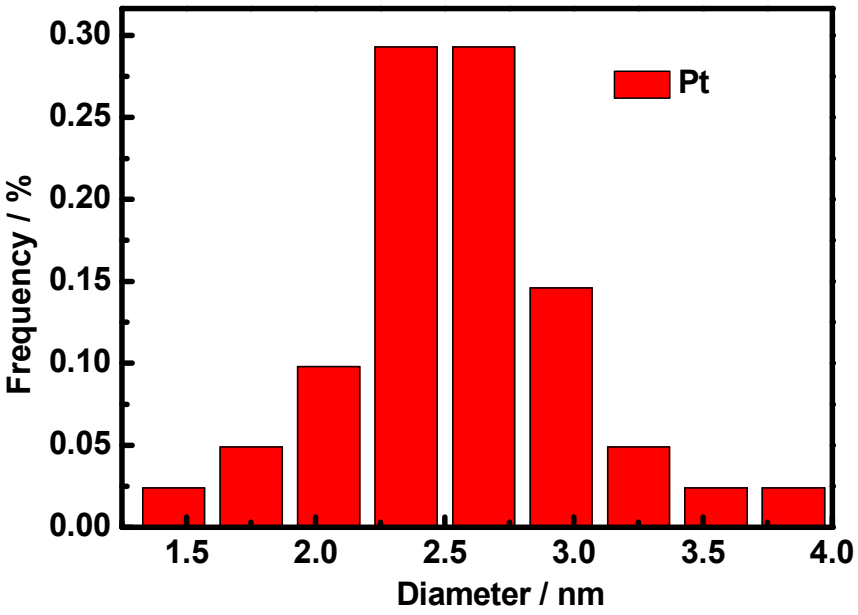

Figure S5. The size distribution histogram of the ligament for the nanoporous Pt on the $(Mn,Al)_3O_4$ substrate based on the TEM image (**Figure 1c**). The average ligament size is about 2.6 nm.

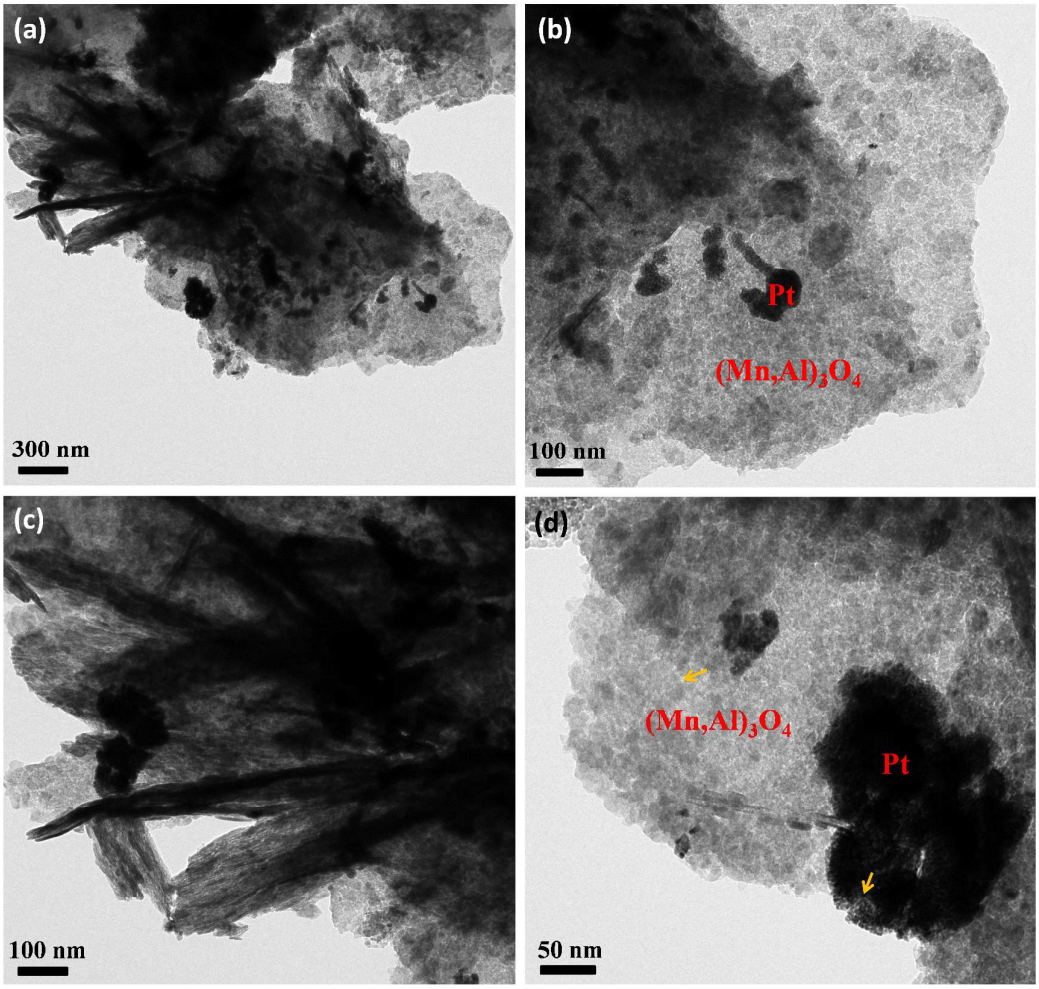

Figure S6. (a-d) The TEM images of the np-Pt/$(Mn,Al)_3O_4$ NS sample. From the above images, it is clear to see that the polygonal nanosheet morphology of the $(Mn,Al)_3O_4$ substrate and nanoporous Pt dispersed on the $(Mn,Al)_3O_4$ substrate.

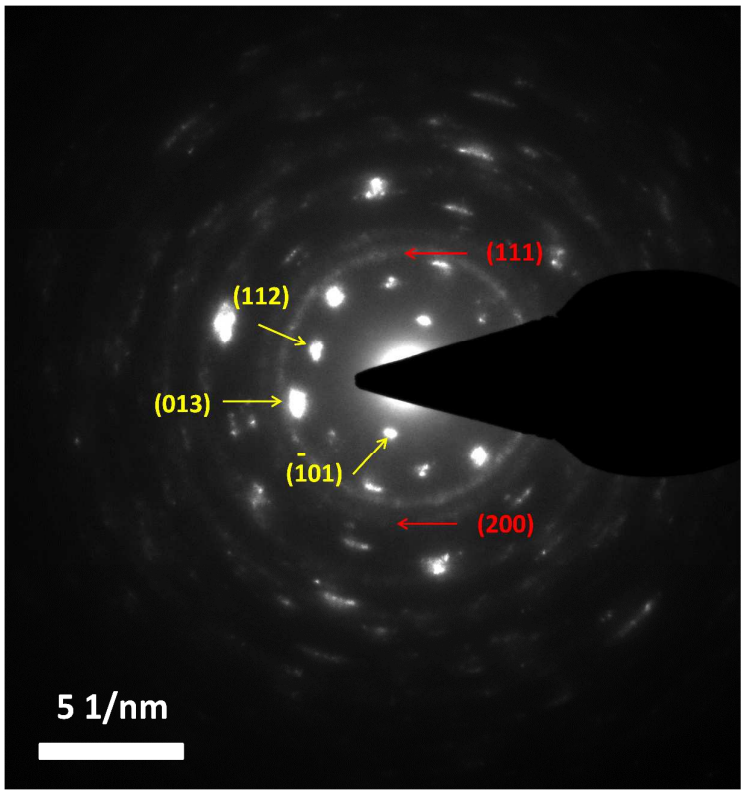

Figure S7. SAED pattern of the np-Pt/$(Mn,Al)_3O_4$ NS sample. The bright diffraction spots indicate the single crystalline nature of $(Mn,Al)_3O_4$ and the diffraction rings agree well with the nanocrystalline nature of np-Pt.

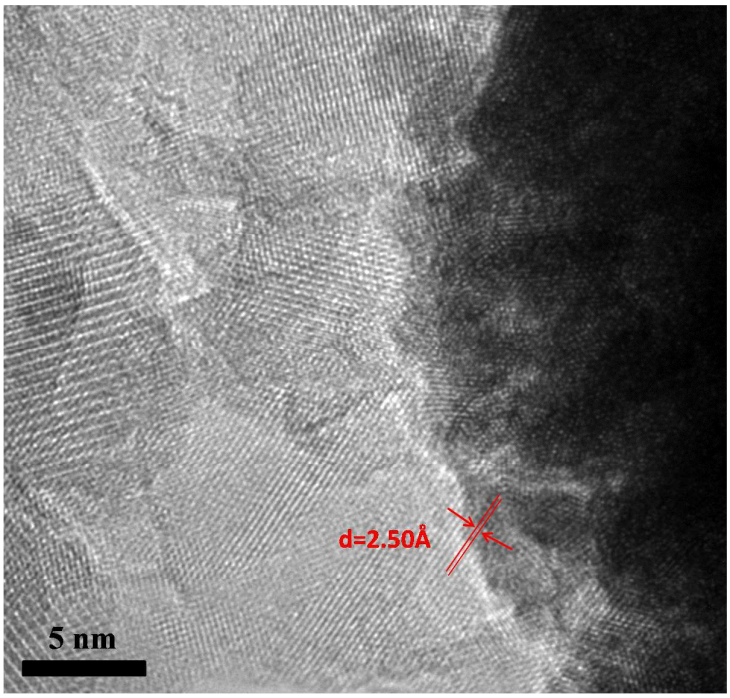

Figure S8. HRTEM image of the np-Pt/$(Mn,Al)_3O_4$ NS sample. From this figure, it is clearly to see that nanoporous Pt has obvious coherent relationship with the $(Mn,Al)_3O_4$ substrate.

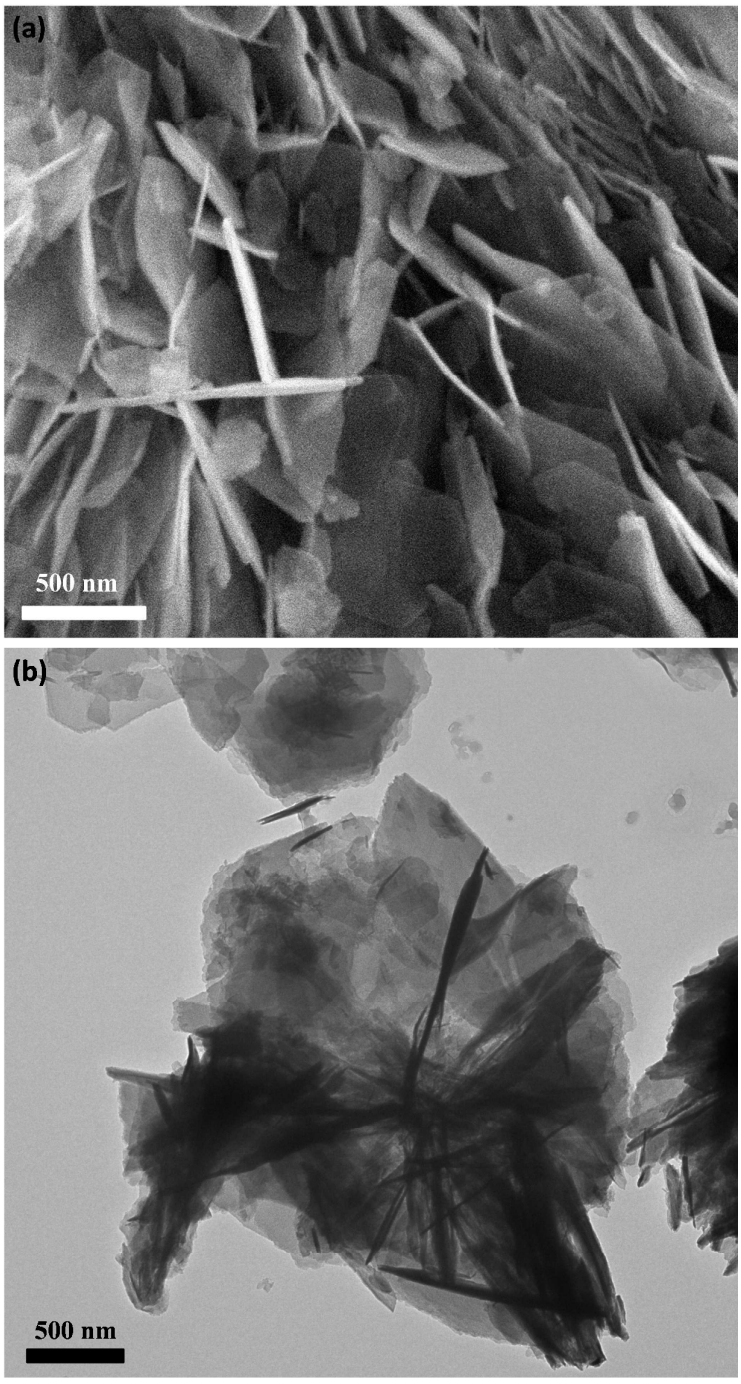

Figure S9. (a) SEM image of the $(Mn,Al)_3O_4$ sample. (b) TEM image of the $(Mn,Al)_3O_4$ sample.

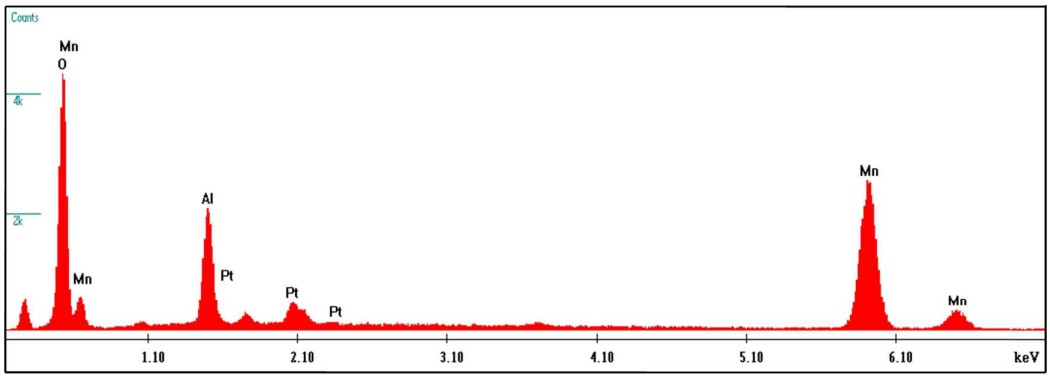

Figure S10. SEM-EDX spectrum of the np-Pt/$(Mn,Al)_3O_4$ NS sample. The mass fraction of Pt in the np-Pt/$(Mn,Al)_3O_4$ NS sample was determined to be 6.52%.

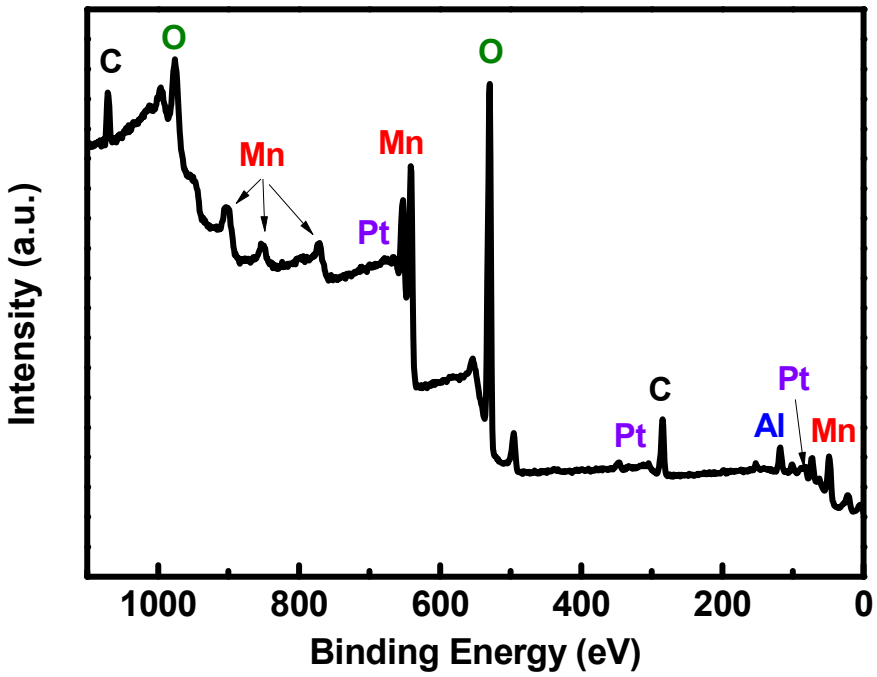

Figure S11. XPS spectrum of the np-Pt/$(Mn,Al)_3O_4$ NS sample.

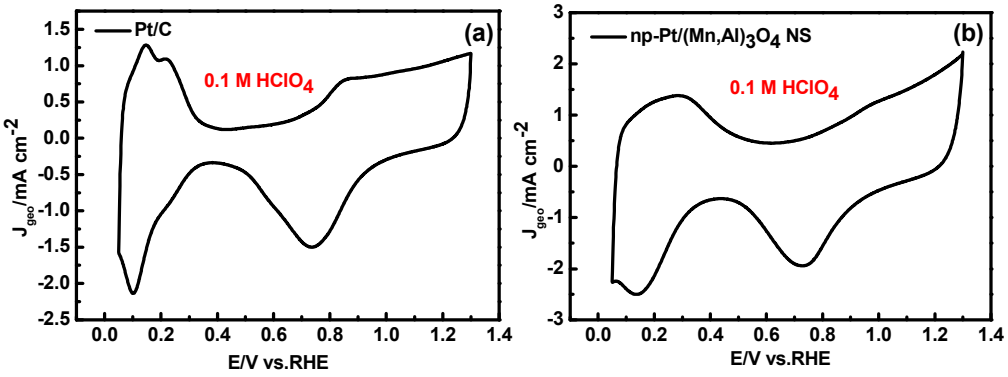

Figure S12. Cyclic voltammetry (CV) curves of the (a) Pt/C and (b) np-Pt/$(Mn,Al)_3O_4$ NS catalysts in the N_2-saturated 0.1 M $HClO_4$ solution at the scan rate of 50 mV s^{-1}.

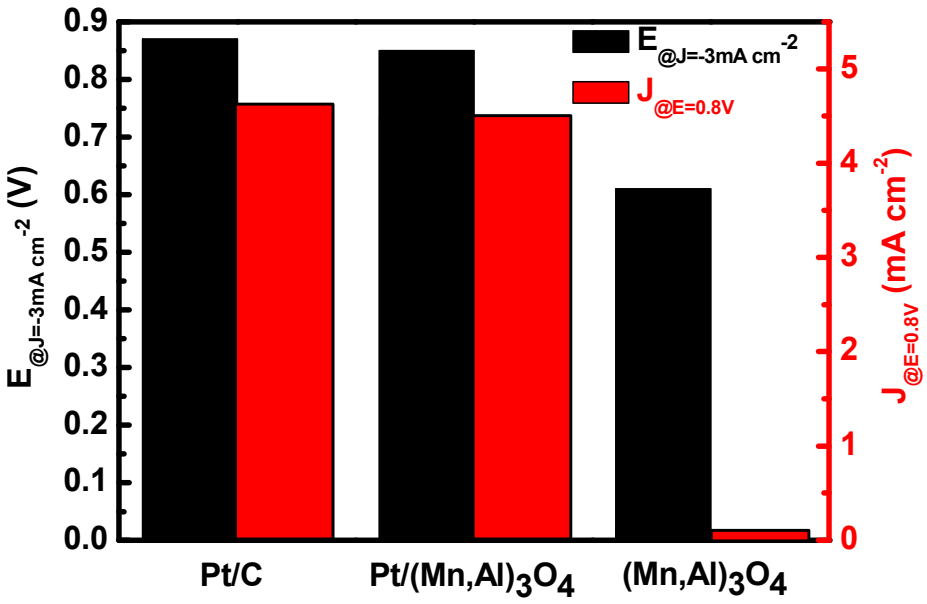

Figure S13. Comparison of $E_{@J= -3\ mA\ cm^{-2}}$ and $J_{@E= 0.8V}$ of the np-Pt/$(Mn,Al)_3O_4$ NS, $(Mn,Al)_3O_4$ and commercial Pt/C catalysts in the 0.1 M KOH solution.

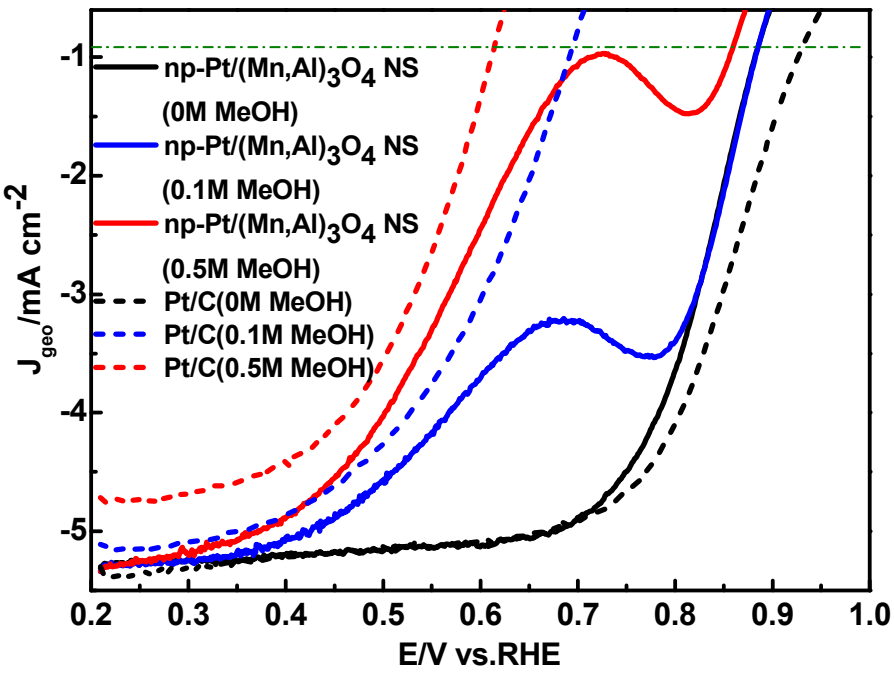

Figure S14. Enlarged plot of polarization curves for ORR on the Pt/C and np-Pt/$(Mn,Al)_3O_4$ NS catalysts in the O_2-saturated 0.1 M KOH electrolyte containing 0, 0.1 and 0.5 M MeOH at 1600 rpm and 10 mV s^{-1}.

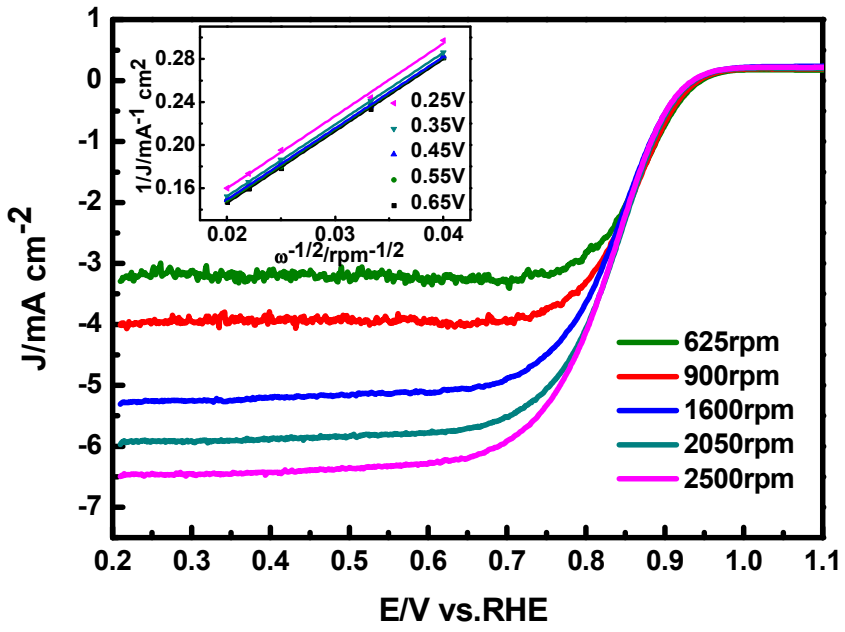

Figure S15. Polarization curves for ORR on the np-Pt/$(Mn,Al)_3O_4$ NS catalyst at various rotation rates in the O_2-saturated 0.1M KOH electrolyte at the scan rate of 10 mV s^{-1}. Inset: Koutecky–Levich plots at different potentials: 0.65, 0.55, 0.45, 0.35 and 0.25V vs. RHE.

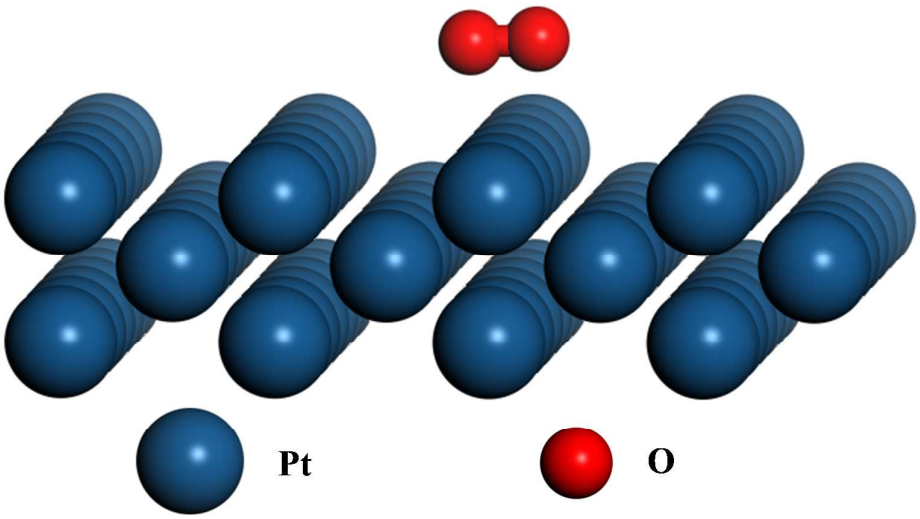

Figure S16. The status of O_2 molecule adsorbed on the Pt (110).

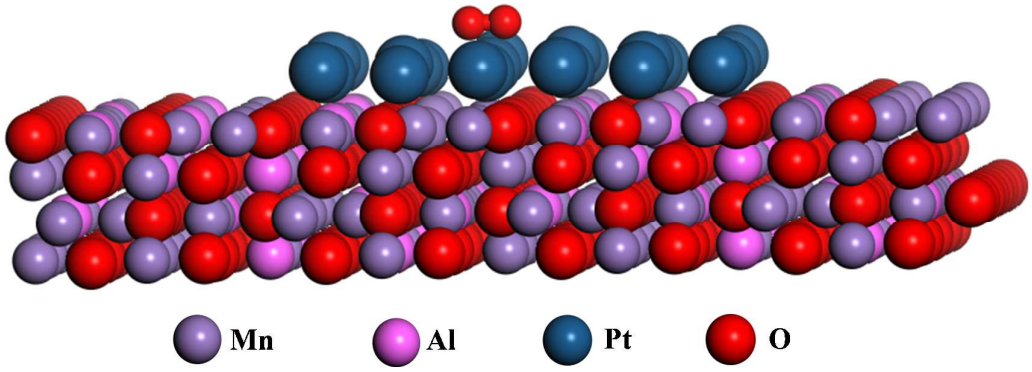

Figure S17. The status of O_2 molecule adsorbed on the np-Pt/$(Mn,Al)_3O_4$ NS (110).

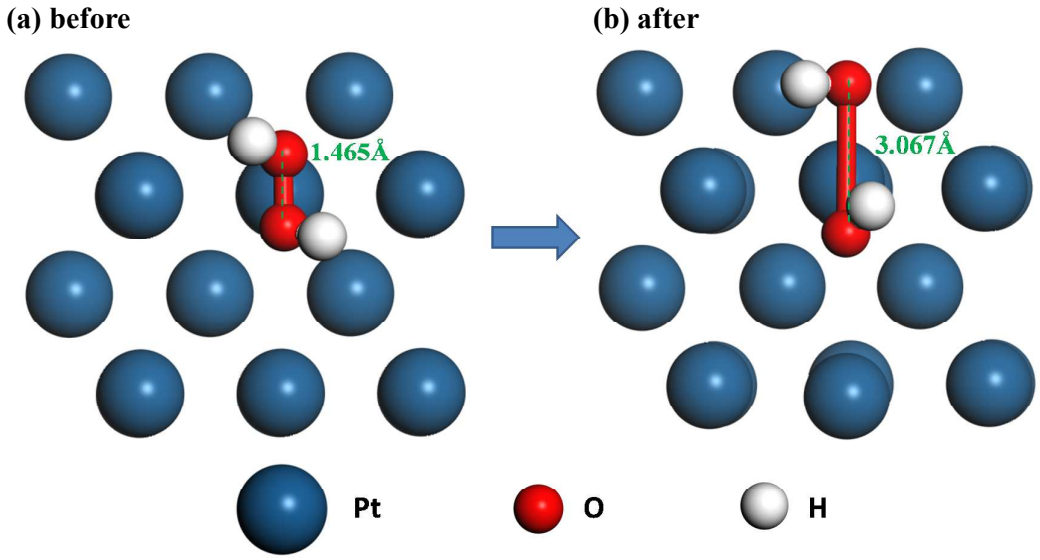

Figure S18. The status of HOOH molecule adsorbed on the Pt (110) (a) before and (b) after optimization.

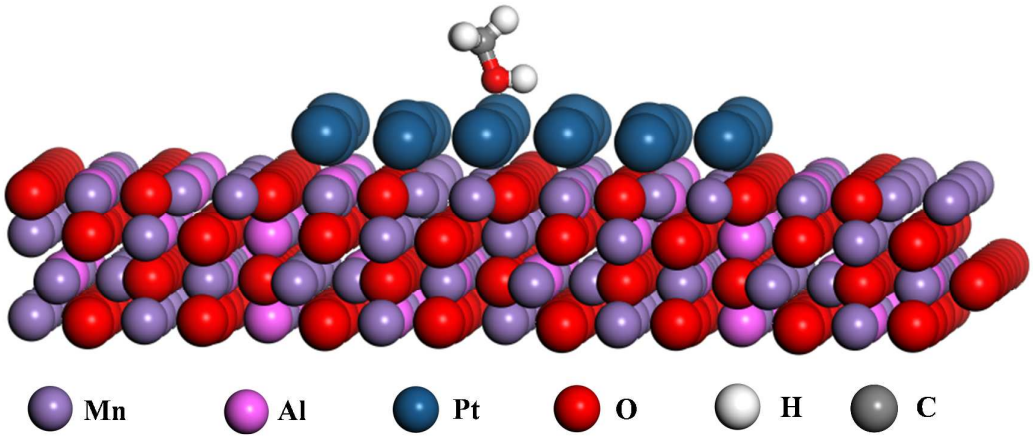

Figure S19. The status of CH_3OH molecule adsorbed on the np-Pt/$(Mn,Al)_3O_4$ NS (110).

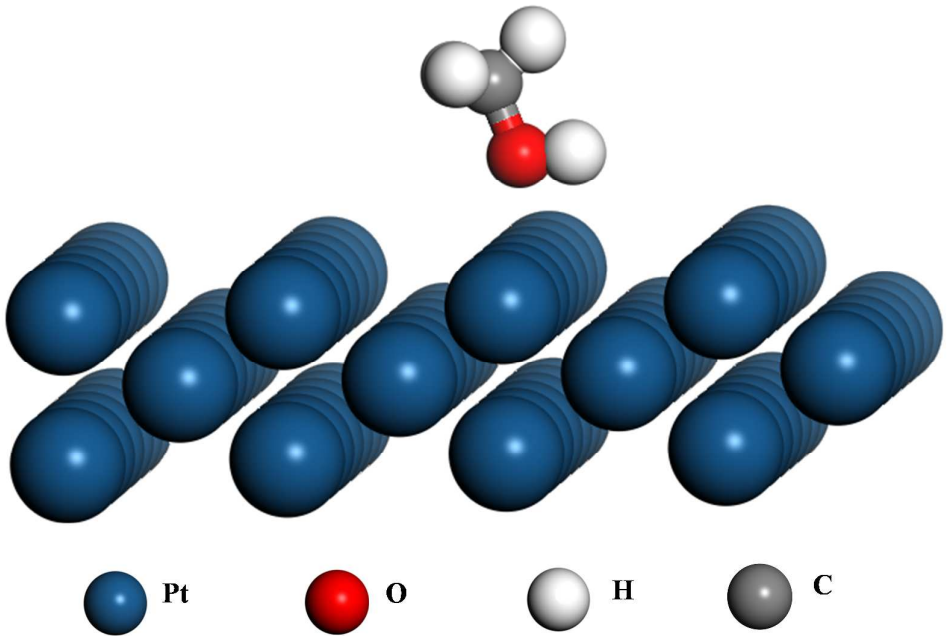

Figure S20. The status of CH_3OH molecule adsorbed on the Pt (110).